Journal of Nuclear Medicine, published on May 10, 2019 as doi:10.2967/jnumed.118.224881

Blocking Glucagon Like Peptide-1 Receptors in the Exocrine Pancreas Improves Specificity for Beta Cells in a Mouse Model of Type 1 Diabetes

Running title – Selective blocking of exocrine GLP-1R

Eshita Khera[1*], Liang Zhang[1*], Sheryl Roberts[2], Ian Nessler[1], Darleen Sandoval[3], Thomas Reiner[2,4,5], and Greg M. Thurber[1,6]

* - these authors contributed equally to the work

[1]Department of Chemical Engineering, University of Michigan, Ann Arbor, Michigan.

[2]Department of Radiology, Memorial Sloan Kettering Cancer Center, New York, New York.

[3]Department of Surgery, University of Michigan Medical School, Ann Arbor, Michigan.

[4]Department of Radiology, Weill Cornell Medical College, 1300 York Avenue, New York, New York.

[5]Chemical Biology Program, Memorial Sloan Kettering Cancer Center, New York, New York 10065

[6]Department of Biomedical Engineering, University of Michigan, Ann Arbor, Michigan.

Keywords: exendin, beta cell mass, exocrine GLP-1R, type-1 diabetes, streptozotocin, mouse model

Corresponding Author: Greg M. Thurber, University of Michigan, 2800 Plymouth Rd., Ann Arbor, MI 48109. Phone: 734-764-8722; Fax: 734-763-0459; E-mail: gthurber@umich.edu

Co-first Authors:

Eshita Khera, University of Michigan, 2800 Plymouth Rd., Ann Arbor, MI 48109. Phone: 734-763-9862; Email: ekhera@umich.edu

Liang Zhang, University of Michigan, 2800 Plymouth Rd., Ann Arbor, MI 48109. Phone: 734-763-9862; Email: liangzha@umich.edu

ABSTRACT

The diabetes community has long desired an imaging agent to quantify the number of insulin-secreting beta (β) cells, beyond just functional equivalents (insulin secretion), to help diagnose and monitor early stages of both type 1 and type 2 diabetes mellitus. Loss in the number of β-cells can be masked by a compensatory increase in function of the remaining cells. Since β-cells only form ~1% of the pancreas and decrease as the disease progresses, only a few imaging agents, such as exendin, have demonstrated clinical potential to detect a drop in the already scarce signal. However, clinical translation of imaging with exendin has been hampered by higher than expected pancreatic uptake in subjects with long-term diabetes who lack β-cells. Exendin binds glucagon-like peptide 1 receptor (GLP-1R), previously thought to be expressed only on β-cells, but recent studies report low levels of GLP-1R on exocrine cells, complicating β-cell mass quantification. Here we use a GLP-1R knockout mouse model to demonstrate that exocrine binding of exendin is exclusively via GLP-1R (~1,000/cell), and not any other receptors. We then use lipophilic Cy-7 exendin to selectively pre-block exocrine GLP-1R in healthy and streptozotocin-induced diabetic (STZ) mice. Sufficient receptors remain on β-cells for subsequent labeling with a fluorescent- or 111In-exendin, which improves contrast between healthy and diabetic pancreata, and provides a potential avenue for achieving the long-standing goal of imaging β-cell mass in the clinic.

INTRODUCTION

Type 1 Diabetes Mellitus, hereafter referred to as 'diabetes', is an autoimmune condition characterized by insulin-deficient hyperglycemia from immune-mediated destruction of beta (β) cells. Given the significant delay between β-cell loss and onset of hyperglycemia (*1*) and the excess capacity of insulin secreting cells, isolating the impact of β-cell function from total β-cell mass (BCM) in the clinic is challenging. Current BCM detection approaches are indirect, (e.g. measuring C-peptide), and cannot distinguish between a large BCM with low secretion and a small BCM with high secretion (e.g. a 'honeymoon phase' (*2*)). Consequently, there is a critical need for direct and non-invasive mapping of BCM changes for early disease screening and progression monitoring. Molecular imaging of β-cells is a promising approach for measuring BCM but presents several unique challenges. β-cells constitute only a small fraction of the pancreas (1-2% cells), and are organized in Islets of Langerhans ~30-400 μm in diameter (*3*) which are below the resolution of clinical scanners. Combined with partial volume effects, the detectable signal from BCM is attenuated nearly 100-fold(*3*), even in healthy subjects.

Despite these hurdles, several probes directed towards β-cell markers have recently progressed to large animal and clinical studies (*4,5*), broadly classified as either functional or BCM probes. Functional probes cannot distinguish healthy BCM from a residual fraction of functionally overcompensating β-cells in the early stages of diabetes where treatment intervention may be most effective (*1*). Quantitative BCM probes can measure total BCM rather than only functionally active β-cells, and exendin probes directed against GLP-1R (glucagon-like peptide-1 receptor) (*6*) have emerged as promising candidates, possessing ideal imaging agent properties (*7*). Yet, advanced pre-clinical and clinical success for imaging has been surprisingly limited due to higher than expected off-target pancreatic uptake in subjects with long-term diabetes.

GLP-1R on non-β cells could explain the lack of clinical distinction between healthy volunteers and subjects with long-term diabetes using exendin-based probes (*8*). While initially controversial due to cross-reactive antibodies combined with low absolute expression, several groups have verified measurable

exocrine GLP-1R expression (*8-20*). Species-dependent variability in exocrine-to-islet signal ratio (*17,21*) (Table 1) highlights additional challenges with evaluating exendin-based probes in animal models. We previously found ~50-fold lower (accessible) GLP-1R expression on mouse exocrine cells compared to β-cells (*16*), mediating significant non-β cell uptake. Since poor clinical contrast is a key barrier to successful BCM imaging, we sought to address this issue using a quantitative approach. In this study, using a GLP-1R knockout mouse model, we demonstrate that exocrine uptake of exendin is exclusively via GLP-1R. Furthermore, using a diabetes mouse model, we demonstrate as a proof-of-concept that selective blocking of exocrine GLP-1R using a slow-clearing exendin variant enables 111In-exendin to bind exclusively to β-cells, thereby providing higher specificity and accuracy for BCM quantification. With optimization and clinical measurements of GLP-1R expression, this strategy could potentially be translated to the clinic for quantifying subtle changes in BCM for pre-symptomatic diabetes detection and pre-treatment disease monitoring.

METHODS AND MATERIALS

Materials

All chemicals, unless specified, were purchased from Sigma Aldrich (Milwaukee, WI). Peptide and reaction details are provided in Supplemental Fig. 1 (*16,22*). All animal experiments were conducted under the approval of the Institutional Animal Care and Use Committee (IACUC) at the University of Michigan and Memorial Sloan Kettering Cancer Center and followed the National Institutes of Health guidelines for animal welfare. Healthy C57Bl/6J and streptozotocin-induced (STZ) diabetic C57Bl/6J mice (6-8 weeks) were purchased from Jackson Laboratory (Bar Harbor, ME). Previously validated(*23*) GLP-1R knockout C57Bl/6J mice (6-8 weeks) were used. Exendin conjugates were dosed intravenously via tail vein catheters.

GLP-1R Knockout Experiments

To probe the specificity of interaction between GLP-1R and exendin, healthy and GLP-1R knockout C57Bl/6J mice were administered 1 nmol of 647-exendin either alone or preceded by a 15-fold

excess pre-block dose of unlabeled exendin for 10 min (N=3 for each of the 4 conditions). After 20 min, the mice were euthanized, and the pancreas was resected. Each pancreas was imaged macroscopically using a Licor Odyssey CLx imager (Lincoln, NE) to confirm successful islet targeting/blocking. Pancreata were then digested in 1000 U/ml collagenase IV for 15 minutes at 37ºC with intermittent shaking. The digest solution was filtered with a 40 μm filter to generate a single cell suspension and washed twice with cell media and PBS. Lastly, cells were fixed in 4% paraformaldehyde, permeabilized, and stained for insulin using a rabbit anti-insulin primary and a goat anti-rabbit fluorescein isothiocyanate secondary antibody. Data were quantified using the Attune Acoustic Focusing Flow Cytometer (ThermoFisher, Waltham, MA) and analyzed using FlowJo. Events were gated for whole cells, followed by single cells, and finally for insulin positive or negative cells to distinguish distinct exocrine and β-cell populations. Statistical analysis using *Student's t test* was performed on GraphPad Prism.

Selective Blocking of Exocrine GLP-1R

Each experiment consisted of a set of three mice administered with a '*Label*' dose, '*Low block*' dose or '*High block*' dose of the exendin conjugates(s) (N >=3) in healthy and streptozotocin-diabetic C57Bl/6J mice (Table 2). Dosing schedule was optimized using modeling and experimental studies, accounting for previously observed exendin and receptor kinetics (*7,16*). For the 'Low block' group, a final 15nmol wt-exendin dose (Dose3) was administered to 'quench' any newly synthesized/recycled GLP-1R and prevent unwanted uptake during probe washout from the blood. At each endpoint, the mice were euthanized, and the pancreas resected. For mice administered 647-exendin, the pancreas was processed similar to the GLP-1R knockout mice.

For mice administered 111In-exendin (Supplemental Table 1), the pancreata were resected and immediately exposed to a digital phosphor autoradiography plate overnight using a GE Healthcare Typhoon FLA 7000 (Port Washington, NY). Serial sections were used for immunohistochemistry to confirm tissue identity and insulin levels. *Ex vivo* biodistribution of 111In-exendin in healthy and streptozotocin-diabetic mice was performed. Briefly, blood and relevant organs were resected, weighed and the radioactivity from

each organ counted in a Wizard automatic γ-counter (PerkinElmer, Boston, MA). The organ accumulation was expressed as a percentage of injected dose per gram (%ID/g).

Histology and Microscopy

'*Low block*' pancreata were embedded in OCT and flash-frozen in 2-methylbutane chilled using dry ice. 5 μm pancreas sections were fixed with 4% paraformaldehyde for 10 minutes at room temperature and stained overnight at 4 ^{o}C with a rabbit anti-insulin primary antibody (1:150 in PBS with 0.1% BSA). Sections were then incubated with goat anti-rabbit-AF555 secondary antibody (1:200 in PBS with 0.1% BSA) for 30 minutes at room temperature. Stained slices were imaged using Olympus FV 1200 Confocal Microscope and analyzed on ImageJ.

RESULTS

Exendin Uptake in Exocrine Pancreas is Exclusively Via GLP-1R

Macroscopic pancreas scans (Fig. 1A) demonstrated the presence of bright, punctate spot formation in WT group administered 647-exendin only, consistent with strong targeting of β-cells in islets of Langerhans. Pre-blocked WT and both KO groups did not form punctate spots, visually confirming the lack of interaction between GLP-1R and 647-exendin, either due to complete blocking or absence of GLP-1R. Quantitative single-cell analysis of exendin uptake by flow cytometry (Fig. 1B) demonstrated strong targeting of 647-exendin to endocrine (β) cells in the labeled WT group, which diminished ~40-fold with both a pre-block dose and when administered in KO mice, consistent with the exclusive interaction between exendin and GLP-1R on β-cells. Comparatively, single-cell exocrine pancreas in labeled WT group showed low yet robust 647-exendin targeting, which was also diminished with pre-block exendin, indicating significant receptor-mediated binding on exocrine pancreas cells. Conversely, exocrine signal from both KO groups was statistically nonsignificant from WT pre-blocked exocrine autofluorescence. The GLP-1R KO model has fully functional islets with abrogated expression of only GLP-1R, while a non-fluorescent exendin dose blocks GLP-1R and any other cross-reacting receptors. Therefore, if exendin binding was not

exclusive to GLP-1R, the exocrine signal from labeled GLP-1R KO cells would have been higher than WT and GLP-1R pre-blocked cells. These results indicate that exendin binds exocrine pancreas exclusively via GLP-1R.

Single-cell Resolution of Selective Exocrine GLP-1R Blocking

Direct administration of labeled exendin leads to binding of GLP-1R on both β-cells and exocrine cells. Although the differential *in vivo* expression between endocrine and exocrine cells is significant (54,000 GLP-1R per β-cell in C57Bl6/J mice(*16*) versus 1,400 GLP-1R per exocrine cell), the higher prevalence of exocrine cells can dramatically skew BCM quantification (*16,21*), since limited spatial resolution of current imaging modalities cannot distinguish between β-cell signal and exocrine signal (Fig. 2A). Considering receptor expression levels, we hypothesized that a calibrated pre-block dose of a slow-clearing Cy7-exendin could selectively occupy the scarce GLP-1R on exocrine cells, while leaving sufficient GLP-1R on β-cells available for binding to the imaging probe, and therefore accurately monitor the BCM loss (Fig. 2B).

Macroscopic scans of 647-exendin group (Supplemental Fig. 2) showed bright punctate islets in healthy '*Label*' pancreas which were absent in healthy '*High Block*' and streptozotocin-diabetic '*Label*', consistent with blocked or absent islets. Scans of healthy '*Low Block*' pancreas still showed punctate islets, a promising indicator that pre-blocking with low Cy7-exendin does not block all GLP-1R on β-cells. Flow cytometry analysis of the pancreata showed strong 647-exendin targeting in the small fraction of β-cells in healthy **'***Label*' pancreas, while healthy '*Low Block*' pancreas showed a distinct (but decreased) β-cell signal compared to complete blocking in the healthy '*High Block*' pancreas (Fig. 3A). The tall exocrine peak for *'Label'* is a statistically higher ($p < 0.05$) than either '*Low Block*' or '*High Block*', in both healthy and streptozotocin-diabetic mice (Fig. 3B), demonstrating that direct labeling can significantly confound β-cell detection. By selectively blocking exocrine GLP-1R over β-cell GLP-1R, a '*Low Block*' Cy7-exendin dose provides the best resolution for quantifying differences in β-cell mass between a healthy and diabetic pancreas (Fig. 3C).

Selective Blocking Improves Resolution of BCM Quantification Using 111In-exendin

Since PET-imaging of exendin in the pancreas is impractical in mice, 111In was selected over PET-probes like 68Ga for its longer half-life and ease of use for autoradiography, in addition to low background binding and high sensitivity. Whole pancreas scans of 111In-exendin '*Label*' streptozotocin-diabetic pancreata showed reduced radioactivity compared to healthy pancreata consistent with the lack of β-cells, but still exhibited high diffuse signal, indicating non-targeted exocrine uptake (Fig. 4A). '*High block*' pancreata exhibited low radioactivity in healthy and streptozotocin-diabetic mice (except when contaminated with fat tissue), re-affirming GLP-1R expression on exocrine cells. '*Low Block*' healthy pancreata exhibited reduced, but measurable radioactivity while the '*Low block*' streptozotocin-diabetic pancreata showed no radioactivity (similar to healthy '*Cy7-High block*' and streptozotocin-diabetic '*High block*') highlighting the improved contrast between healthy and diabetic mice from selective blocking using Cy7-exendin. Histology confirmed the difference in number and size of insulin-positive islets between healthy and streptozotocin-diabetic mice (Fig. 4B; Supplemental Fig. 3). Quantitatively, 111In -exendin uptake in '*Label*' streptozotocin-diabetic pancreas was only 1.7-fold lower than '*Label*' healthy pancreas, even though the former does not contain any β-cells. However, the contrast increased to 9.6-fold between '*Low block*' healthy and streptozotocin-diabetic pancreas, providing enhanced resolution of β-cell detection (Fig. 5A). This is in agreement with the sharp (~12-fold) reduction in 111In-exendin uptake in '*Low Block*' and '*High Block*' streptozotocin-diabetic pancreata ($p < 0.005$), highlighting the potential for low Cy7-exendin to block all exocrine GLP-1R. The healthy '*Low Block*' pancreas exhibits 111In-exendin uptake intermediate to the '*Label*' and '*High Block*' pancreata, consistent with complete blocking of exocrine GLP-1R but only partial β-cell GLP-1R blocking (Fig. 5B). 111In-exendin uptake in healthy and streptozotocin-diabetic '*High block*' groups was slightly higher than expected (*ns*) in healthy '*High block*' (Fig 5B), likely due to rapid clearance of wt-exendin prior to 111In-exendin. Full organ biodistribution is included in Supplemental Fig. 4 (*24,25*).

For this proof-of-concept study, the Cy7-exendin dose was optimized to err on the side of complete exocrine blocking, even at the cost of blocking more β-cell GLP-1R. Consequently, the difference in mean

signal between healthy '*Low block*' and streptozotocin-diabetic '*Low block*' improved to 9.6-fold (Fig. 5A) but was not statistically significant. The majority of healthy '*Low Block*' pancreata were higher than completely blocked signal – however, two of these were very high (2.4 and 2.6 %ID/g). Though ideal, these two data points increased the standard deviation for healthy *'Low block'* mice and drove the lack of statistical significance. If these two values are excluded, the resulting difference between '*Low block*' healthy and streptozotocin-diabetic pancreata is still better than no blocking dose (3.6-fold with *'Low Block'* versus 1.7-fold difference with '*Label*') and it is statistically significant ($p < 0.05$) (Supplemental Fig. 5). Additional fine-tuning of the Cy7-exendin dose in future studies may help alleviate this variability.

DISCUSSION

Quantifying beta cell mass is an important goal in diabetes research, and exendin-based probes have many optimal properties. However, recent evidence shows low-level GLP-1R on exocrine cells, and this confounding effect from non-target cells is a primary hurdle for clinical translation of exendin for BCM quantification. In this study, we confirm that GLP-1R alone is responsible for the exocrine uptake. Additionally, our quantitative measurements show in a diabetes mouse model that selective exocrine GLP-1R blocking with a low cold-dose of lipophilic exendin can enhance the resolution of β-cells to distinguish healthy from diabetic pancreas.

Cold-dose blocking is routinely used in cancer imaging (*26-28*) for preferential blocking of receptors in healthy tissue to improve contrast, facilitated by efficient normal tissue uptake relative to poor tumor delivery. However, preferential blocking of exocrine over β-cells is more challenging, as they are in the same well-perfused pancreas. The blood vessel surface area to volume ratio (i.e. delivery) is 3-fold higher in the islets compared to exocrine tissue (*3,29*); thus a sub-saturating cold-block dose would theoretically block 3-fold more β-cell receptors than exocrine receptors. Eriksson *et al.* found 4- and 5-fold higher exendin uptake in islets in mice and non-human primates, respectively (*21*), indicating additional factors like diffusion from the surrounding exocrine (similar to micrometastases (*29*)) could impact cold-dose blocking of exocrine GLP-1R. Additionally, receptor recycling is a critical consideration, and selective

blocking of exocrine blocking requires blocking both extracellular and intracellular reserves of exocrine GLP-1R with the pre-block dose (Supplemental Fig. 6). To overcome these challenges, we utilized a lipophilic Cy7-exendin for blocking – first, to slow plasma clearance (*16,22*) and block both extracellular and intracellular stores of exocrine GLP-1R (*30*). Second, the lipophilic Cy7 moiety slows exendin diffusion compared to hydrophilic exendin (Supplemental Fig. 7) (*16,21,31*), which limits its diffusion into islets from the surrounding exocrine tissue (Supplemental Fig. 8). Indeed, the use of unlabeled (hydrophilic) wt-exendin as the low pre-block dose did not block exocrine GLP-1R as selectively as lipophilic Cy7-exendin (*data not shown*). Finally, the use of a lipophilic cyanine dye allowed tracking of the blocking probe if needed, while the similarity to the FDA-approved liraglutide (GLP-1 analog attached to a fatty acid instead of lipophilic Cy7) provides a potential path for translation. Though the doses employed here are higher than therapeutic doses of liraglutide, several reports of extremely high doses pose no safety issues/side effects besides nausea (resolved with anti-emetics (*32,33*)). The systemic clearance of Cy7-exendin is faster than that of IgGs commonly used in cold-dose blocking, enabling repeat imaging if necessary. For clinical translation, the difference in expression between human exocrine and beta cells needs to be sufficient to allow for selective blocking. This dosing 'window' will compensate for variability in plasma clearance of the blocking dose by maintaining complete exocrine blocking while retaining sufficient beta cell GLP-1R to provide an excess of receptor for tracer probe binding.

In theory, a pre-blocking dose could reduce variability in human pancreas signal by eliminating the variable exocrine uptake, but differences in the pharmacokinetics of the pre-blocking dose have the potential to increase signal variability as well. Therefore, selection of an optimal blocking dose is critical – too high of a dose will block all GLP-1R, while too low will leave exocrine GLP-1R unblocked. Here, we erred on the side of complete exocrine blocking at the cost of more endocrine blocking/variability. Further dose tuning could improve imaging resolution, but clinical translation depends on relative islet-to-exocrine expression/delivery in humans and potential consideration of islet architecture (*34*). The differences in architecture, however, are unlikely to be significant given the extremely low penetration distance of lipophilic exendin (10μm) compared to hydrophilic exendin (70μm) (Supplemental Fig. 8). Promisingly,

endocrine/exocrine expression appears similar between mice and humans (*ex vivo* islet-to-exocrine ratio ~ 2-7 in humans (*9,11,19*), ~3 in mice (*35*), ~5 in monkey (*36*) , and > 30 in rat (*9*)). However, histology doesn't capture delivery limitations and receptor trafficking present *in vivo*, requiring further assessment.

The use of radiolabeled PET/SPECT-based probes for BCM quantification is a contentious field, with concerns that relatively poor spatial resolution is a substantial limitation for accurate β-cell imaging. Since exocrine pancreas also expresses GLP-1R, PET/SPECT cannot distinguish if the radioactivity is originating from β-cells or exocrine cells, thereby skewing the accuracy of BCM quantification (*37,38*). However, as Gotthardt *et al*. point out, the key influencing factor for successful β-cell quantification using PET is not spatial resolution but ensuring that the radioactive signal observed is exclusively from β-cells (*39*). The use of lipophilic Cy7-exendin in this study achieves this precise BCM specificity by selectively blocking exocrine GLP-1R, thereby allowing the 111In-exendin binding only to β-cell GLP-1R. Thus, this dosing approach eliminates the confounding effects of exocrine uptake that has impeded the successful clinical translation of exendin imaging agents and achieves strong resolution of the BCM. Future developments of this method should focus on incorporation of PET-imaging to evaluate clinical feasibility for β-cell imaging, which was not feasible in this proof-of-principle study due to small size of the organs and proximity of the kidneys relative to the diffusion distance of positrons in mice.

CONCLUSION

We present a novel approach of employing exendin conjugates to improve the specificity of imaging β-cells to quantify BCM, despite the expression of GLP-1R on exocrine pancreas. Using a low pre-block dose of slow-clearing lipophilic Cy7-exendin, we show specific targeting of a 647-exendin imaging probe to β-cells with single-cell resolution and a nearly 6-fold improvement in β-cell versus exocrine uptake of 111In-exendin between healthy and diabetic mouse pancreata compared to administration of the imaging agent alone. With additional fine-tuning and scaling of the selective blocking dose for expression, vascular density, and plasma clearance in humans, this imaging approach could serve

as a potential foundation for clinical application that combines the sensitivity of PET with the strong β-cell resolution needed for accurate quantification of BCM.

FINANCIAL DISCLOSURE

T.R. is a co-founder and shareholder of Summit Biomedical Imaging, LLC. No other potential conflicts of interest relevant to this article exist.

ACKNOWLEDGEMENTS

The authors would like to thank Dr. Dan Drucker for providing the GLP-1 receptor knockout mice and Dr. John Williams for assistance in breeding. The authors thank the support of Memorial Sloan Kettering Cancer Center's Animal Imaging Core Facility, Radiochemistry & Molecular Imaging Probes Core Facility and the Molecular Cytology Core Facility. This work was supported by National Institutes of Health grants K01 DK093766 (G.M.T.), R35 GM128819 (G.M.T.), R01 CA204441 (T. R.), R43 CA228815 (T.R.), P30 CA008748, and an NSF graduate research fellowship (I.N.).

KEY POINTS

Question: How do we overcome off-target uptake of diabetes imaging agents due to exocrine GLP-1R expression?

Pertinent Findings: We devised a novel dosing scheme that selectively pre-blocks exocrine GLP-1R over β-cell GLP-1R using a low dose of lipophilic Cy7-exendin. Proof-of-principle evaluation of this dosing scheme in a mouse model of type-1 diabetes confirmed selective exocrine blocking with single cell resolution using a fluorescent exendin imaging agent and improved uptake contrast between healthy and diabetic mouse pancreas using ^{111}In-exendin.

Implications for Patient Care: The study was designed with future translation to PET-imaging in mind, and demonstration of enhanced contrast between healthy and diabetic mouse pancreas by selectively blocking

exocrine GLP-1R paves the way for a potential clinical molecular imaging technique capable of β-cell mass quantification for diabetes screening and progression monitoring.

REFERENCES

1. Atkinson MA, Eisenbarth GS. Type 1 diabetes: New perspectives on disease pathogenesis and treatment. *The Lancet.* 2001;358:221-229.

2. Bowden SA. Partial remission (honeymoon phase) in type 1 diabetes mellitus. *Frontiers in Clinical Drug Research – Diabetes and Obesity.* 2017;4:1-20.

3. Zhang L, Thurber GM. Imaging in Diabetes. In: Lewis JS, Keshari KR, eds. *Imaging and Metabolism*. Cham: Springer International Publishing; 2018:175-197.

4. Wei W, Ehlerding EB, Lan X, Luo Q-y, Cai W. Molecular imaging of β-cells: Diabetes and beyond. *Advance Drug Delivery Reviews.* 2018.

5. Jodal A, Schibli R, Béhé M. Targets and probes for non-invasive imaging of β-cells. *Eur J Nucl Med Mol Imaging.* 2017;44:712-727.

6. Manandhar B, Ahn J-M. Glucagon-like peptide-1 (GLP-1) analogs: Recent advances, new possibilities, and therapeutic implications. *J Med Chem.* 2015;58:1020-1037.

7. Zhang L, Bhatnagar S, Deschenes E, Thurber GM. Mechanistic and quantitative insight into cell surface targeted molecular imaging agent design. *Sci Rep.* 2016;6:25424-25424.

8. Brom M, Woliner-van der Weg W, Joosten L, et al. Non-invasive quantification of the beta cell mass by SPECT with ^{111}In-labelled exendin. *Diabetologia.* 2014;57:950-959.

9. Waser B, Reubi JC. Radiolabelled GLP-1 receptor antagonist binds to GLP-1 receptor-expressing human tissues. *Eur J Nucl Med Mol Imaging.* 2014;41:1166-1171.

10. Waser B, Blank A, Karamitopoulou E, Perren A, Reubi JC. Glucagon-like-peptide-1 receptor expression in normal and diseased human thyroid and pancreas. *Modern Pathology.* 2015;28:391.

11. Körner M, Stöckli M, Waser B, Reubi JC. GLP-1 receptor expression in human tumors and human normal tissues: Potential for in vivo targeting. *J Nucl Med.* 2007;48:736-743.

12. Reubi JC, Perren A, Rehmann R, et al. Glucagon-like peptide-1 (GLP-1) receptors are not overexpressed in pancreatic islets from patients with severe hyperinsulinaemic hypoglycaemia following gastric bypass. *Diabetologia.* 2010;53:2641-2645.

13. Pyke C, Heller RS, Kirk RK, et al. GLP-1 receptor localization in monkey and human tissue: Novel distribution revealed with extensively validated monoclonal antibody. *Endocrinology.* 2014;155:1280-1290.

14. Wewer Albrechtsen NJ, Albrechtsen R, Bremholm L, et al. Glucagon-like peptide 1 receptor signaling in acinar cells causes growth-ependent release of pancreatic enzymes. *Cell Rep.* 2016;17:2845-2856.

15. Hou Y, Ernst SA, Heidenreich K, Williams JA. Glucagon-like peptide-1 receptor is present in pancreatic acinar cells and regulates amylase secretion through cAMP. *Am J Physiol Gastrointest Liver Physiol.* 2016;310:G26-G33.

16. Zhang L, Thurber GM. Quantitative impact of plasma clearance and down-regulation on GLP-1 receptor molecular imaging. *Mol Imaging Biol.* 2016;18:79-89.

17. Willekens SMA, Joosten L, Boerman OC, et al. Strain differences determine the suitability of animal models for noninvasive in vivo beta cell mass determination with radiolabeled exendin. *Mol Imaging Biol.* 2016;18:705-714.

18. Nalin L, Selvaraju RK, Velikyan I, et al. Positron emission tomography imaging of the glucagon-like peptide-1 receptor in healthy and streptozotocin-induced diabetic pigs. *Eur J Nucl Med Mol Imaging.* 2014;41:1800-1810.

19. Kirk RK, Pyke C, von Herrath MG, et al. Immunohistochemical assessment of glucagon-like peptide 1 receptor (GLP-1R) expression in the pancreas of patients with type 2 diabetes. *Diabetes Obes Metab.* 2017;19:705-712.

20. Horsch D, Goke R, Eissele R, Michel B, Goke B. Reciprocal cellular distribution of glucagon-like peptide-1 (GLP-1) immunoreactivity and GLP-1 receptor mRNA in pancreatic islets of rat. *Pancreas.* 1997;14:290-294.

21. Eriksson O, Rosenström U, Selvaraju RK, Eriksson B, Velikyan I. Species differences in pancreatic binding of DO3A-VS-Cys40-Exendin4. *Acta Diabetol.* 2017;54:1039-1045.

22. Zhang L, Navaratna T, Thurber GM. A helix-stabilizing linker improves subcutaneous bioavailability of a helical peptide independent of linker lipophilicity. *Bioconjug Chem.* 2016;27:1663-1672.

23. Scrocchi LA, Brown TJ, MaClusky N, et al. Glucose intolerance but normal satiety in mice with a null mutation in the glucagon-like peptide 1 receptor gene. *Nat Med.* 1996;2:1254-1258.

24. Monazzam A, Lau J, Velikyan I, et al. Increased expression of GLP-1R in proliferating islets of men1 mice is detectable by [68Ga]Ga-DO3A-VS-Cys40-exendin-4 /PET. *Sci Rep.* 2018;8:748-748.

25. Viby N-E, Isidor MS, Buggeskov KB, Poulsen SS, Hansen JB, Kissow H. Glucagon-like peptide-1 (GLP-1) reduces mortality and improves lung function in a model of experimental obstructive lung disease in female mice. *Endocrinology.* 2013;154:4503-4511.

26. Houghton JL, Abdel-Atti D, Scholz WW, Lewis JS. Preloading with unlabeled CA19.9 targeted human monoclonal antibody leads to improved PET imaging with (89)Zr-5B1. *Mol Pharm.* 2017;14:908-915.

27. Boswell CA, Mundo EE, Zhang C, et al. Differential effects of predosing on tumor and tissue uptake of an 111In-labeled anti-TENB2 antibody-drug conjugate. *J Nucl Med.* 2012;53:1454-1461.

28. Dijkers EC, Oude Munnink TH, Kosterink JG, et al. Biodistribution of 89Zr-trastuzumab and PET imaging of HER2-positive lesions in patients with metastatic breast cancer. *Clin Pharmacol Ther.* 2010;87:586-592.

29. Thurber GM, Weissleder R. Quantitating antibody uptake in vivo: Conditional dependence on antigen expression levels. *Mol Imaging Biol.* 2011;13:623-632.

30. Eriksson O, Laughlin M, Brom M, et al. In vivo imaging of beta cells with radiotracers: state of the art, prospects and recommendations for development and use. *Diabetologia.* 2016;59:1340-1349.

31. Tung YC, Hsiao AY, Allen SG, Torisawa YS, Ho M, Takayama S. High-throughput 3D spheroid culture and drug testing using a 384 hanging drop array. *Analyst.* 2011;136:473-478.

32. Nakanishi R, Hirose T, Tamura Y, Fujitani Y, Watada H. Attempted suicide with liraglutide overdose did not induce hypoglycemia. *Diabetes Res Clin Pract.* 2013;99:e3-e4.

33. Bode SF, Egg M, Wallesch C, Hermanns-Clausen M. 10-fold liraglutide overdose over 7 months resulted only in minor side-effects. *J Clin Pharmacol.* 2013;53:785-786.

34. Kim A, Miller K, Jo J, Kilimnik G, Wojcik P, Hara M. Islet architecture: A comparative study. *Islets.* 2009;1:129-136.

35. Waser B, Reubi JC. Value of the radiolabelled GLP-1 receptor antagonist exendin(9-39) for targeting of GLP-1 receptor-expressing pancreatic tissues in mice and humans. *Eur J Nucl Med Mol Imaging.* 2011;38:1054-1058.

36. Pyke C, Heller RS, Kirk RK, et al. GLP-1 receptor localization in monkey and human tissue: novel distribution revealed with extensively validated monoclonal antibody. *Endocrinology.* 2014;155:1280-1290.

37. Alavi A, Werner TJ. Futility of attempts to detect and quantify beta cells by PET imaging in the pancreas: why it is time to abandon the approach. *Diabetologia.* 2018:1-4.

38. Cline GW, McCarthy TJ, Carson RE, Calle RA. Clinical and scientific value in the pursuit of quantification of beta cells in the pancreas by PET imaging. *Diabetologia.* 2018:1-3.

39. Gotthardt M, Eizirik DL, Aanstoot H-J, et al. Detection and quantification of beta cells by PET imaging: why clinical implementation has never been closer. *Diabetologia.* 2018:1-4.

FIGURES WITH LEGENDS

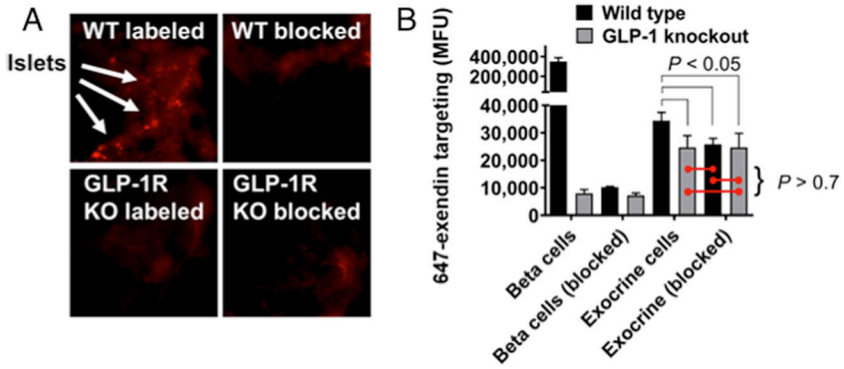

Figure 1. Knockout mouse model demonstrates exclusive exocrine binding of exendin to GLP-1R.

(A) 647-exendin bound islets appear as punctate spots in wild-type (WT) labeled mice, which are absent in WT blocked, GLP-1R knockout (KO) labeled and KO blocked mice.

(B) Quantitative flow cytometry analysis of exocrine pancreas cells shows statistically higher fluorescence in WT labeled mice compared to WT blocked, KO labeled, and KO blocked mice, suggesting binding of exendin to exocrine cells exclusively via GLP-1R.

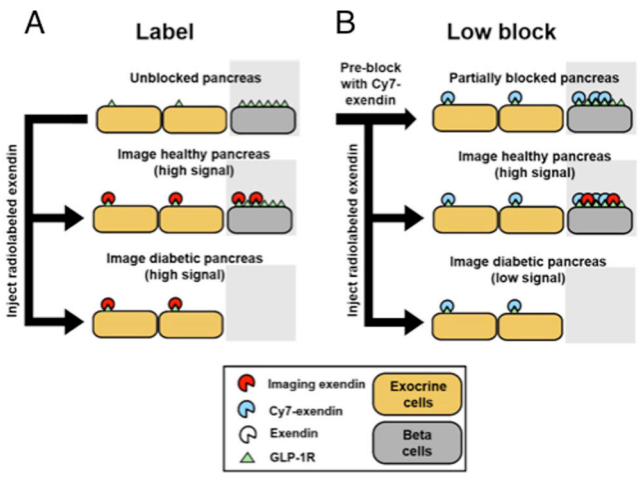

Figure 2. Simplified schematic for β-cell imaging

(A) β-cell quantification resolution using only imaging exendin probe ('*Label*')

(B) Postulated improvement in β-cell quantification resolution using pre-blocked Cy7-exendin followed by imaging exendin probe ('*Low Block*').

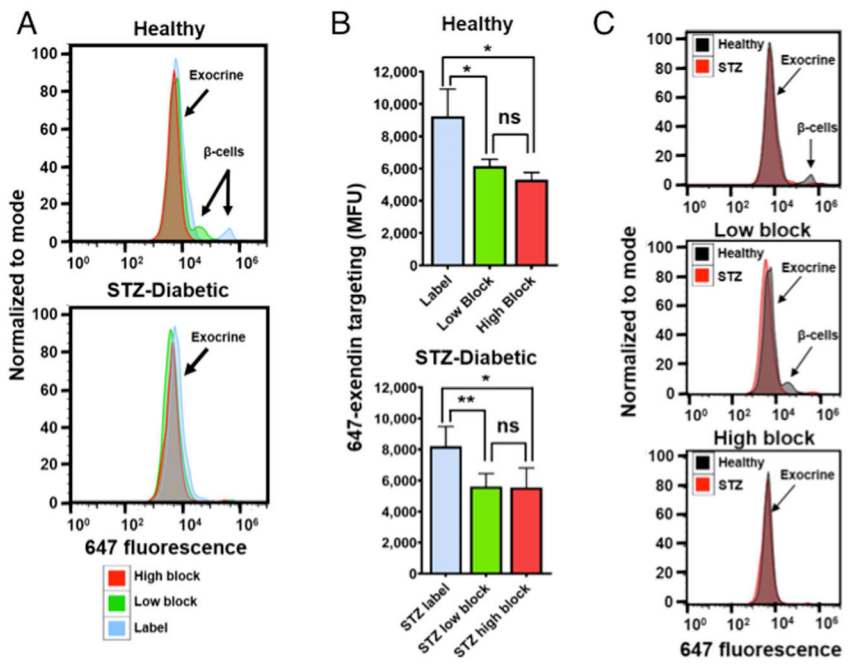

Figure 3. Selective exocrine GLP-1R blocking with single-cell resolution

(A) Fluorescent labeling of the small fraction of β-cells observed in healthy '*Label*' mice is retained in '*Low block*' mice but is completely absent in healthy '*High Block*' and all streptozotocin-diabetic (STZ) mice.

(B) Exocrine GLP-1R is completely blocked in both '*Low block*' and '*High block*' pancreata, in both healthy and streptozotocin-diabetic mice. (*ns* = $p > 0.05$, * = $p < 0.05$, ** = $p < 0.01$)

(C) Healthy versus streptozotocin-diabetic mice highlights improved resolution for detecting β-cell loss.

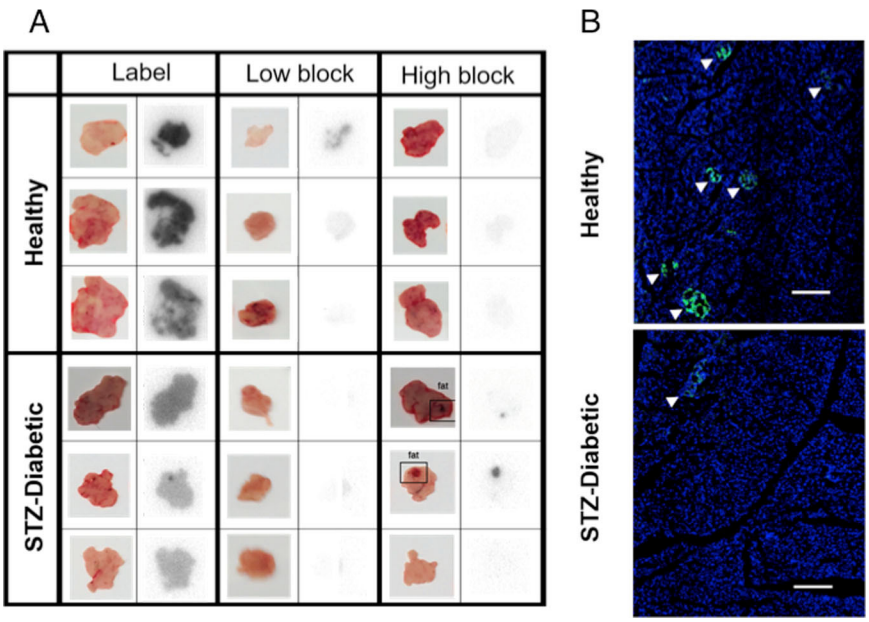

Figure 4. Selective blocking of exocrine GLP-1R isolates islet-specific radioactivity.

(A) Macroscopic autoradiography 111In-exendin injected mice demonstrates binding to exocrine GLP-1R can be abolished using a Cy7-exendin low-block dose or high dose of wt-exendin. The tracer doses are generally not sufficient to see individual islets in thick tissue.

(B) Insulin staining of pancreas slices confirming the presence of numerous large islets in healthy mice that were mostly absent in streptozotocin-diabetic mice (*white arrows*). Scale bar = 250 µm

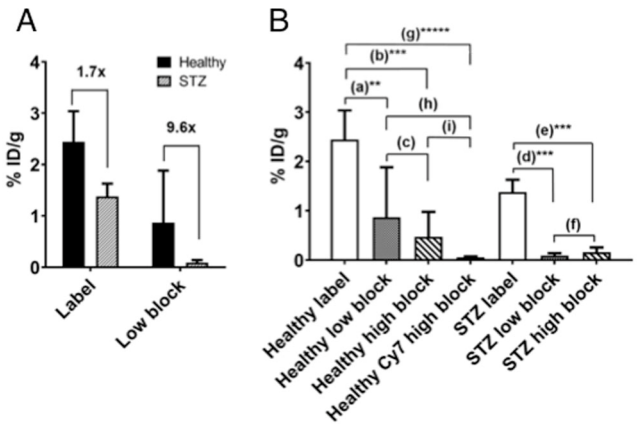

Figure 5. Quantification of β-cell mass (BCM) via selective 111In-exendin uptake.

(A) Pre-blocking with lipophilic Cy7-exendin improves contrast between healthy and streptozotocin-diabetic pancreata 111In-exendin uptake from 1.7 (*) to 9.6 (*ns*), improving the resolution of β-cell imaging. **(B)** Uptake of 111In-exendin in streptozotocin-diabetic mice is reduced with pre-blocking, but lipophilic Cy7-exendin dose retains some uptake in healthy mice, indicating specific targeting of β-cells. Fold differences: *a=2.8, b=5.2, c=1.8, d=15.3, e=8.5, f=0.56, g=43, h=15.3, i = 8.3 (* = p <0.05, ** = p < 0.01, *** = p < 0.005, ***** = p < 0.0005*)

Tables

Table 1. GLP-1R is expressed on exocrine pancreas of most species

Species	Significant Exocrine GLP-1R Expression?	References
Mouse	Yes	(*14-16,21*)
Rat	No	(*8,9,17,20,21*)
Pig	Yes	(*18,21*)
Non-human primate	Yes	(*13,21*)
Human	Yes	(*9-13,19*)

Table 2. Dosing and intervals for selective exocrine GLP-1R blocking.

Fluorescent exendin							
Condition	**Dose and Time Intervals**						
	Dose 1	**Time (min)**	**Dose 2**	**Time (min)**	**Dose 3**	**Time (min)**	
Label	1 nmol 647-exendin	15	Euthanize				
High Block	15 nmol wt-exendin	15	1 nmol 647-exendin	15	Euthanize		
Low Block	7.39 pmol/g Cy7-exendin	10	1 nmol 647-exendin	5	15 nmol wt-exendin	10	Euthanize
Radiolabeled exendin							
Condition	**Dose and Time Intervals**						
	Dose 1	**Time (min)**	**Dose 2**	**Time (min)**	**Dose 3**	**Time (min)**	
Label	2.1 ng 111In -exendin	60	Euthanize				
High Block	15 nmol wt-exendin	15	2.1 ng 111In-exendin	60	Euthanize		
Low Block	7.39 pmol/g Cy7-exendin	10	2.1 ng 111In -exendin	5	15 nmol wt-exendin	55	Euthanize

Supplemental Data

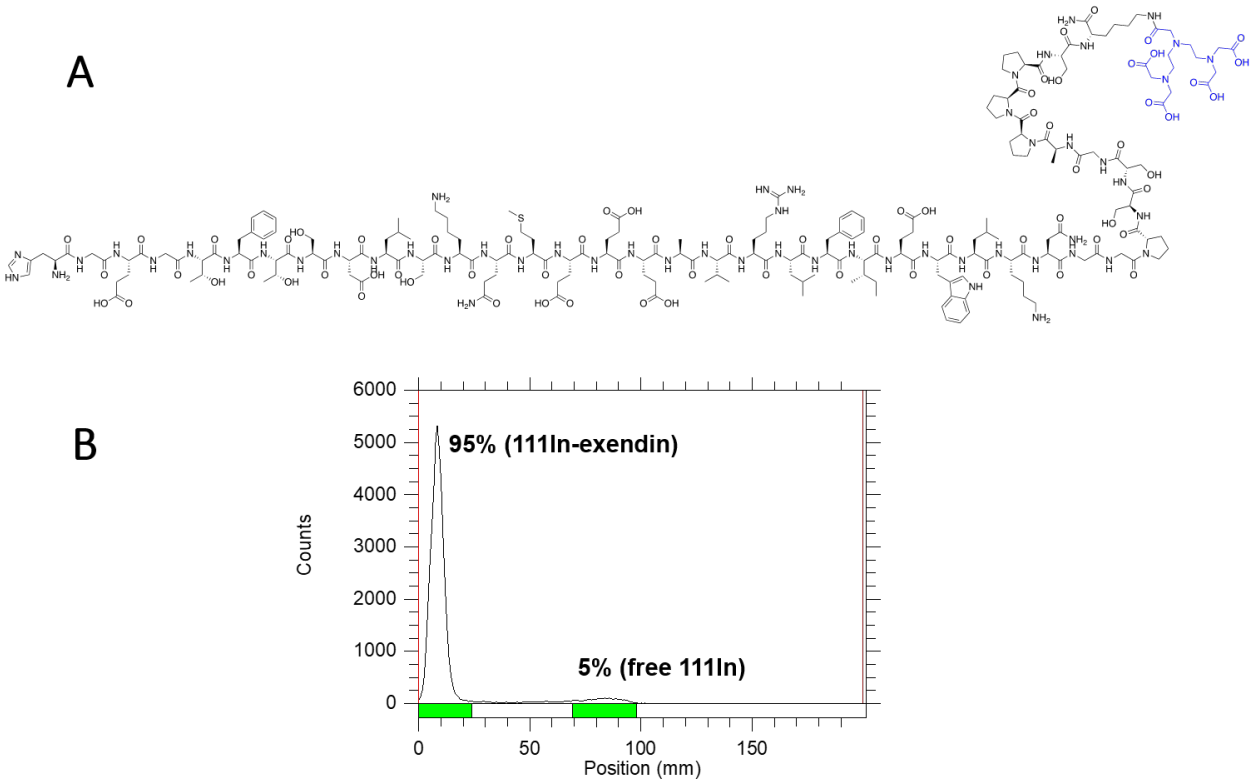

Supplemental Figure 1. Preparation of radiolabeled exendin conjugate (Lys^{40}(^{111}In-DTPA) exendin-4). (A) Structure of Lys^{40}(^{111}In-DTPA) - (DTPA)] exendin-4. Wild-type exendin-4 (H-HGEGTFTSDLSKQMEEEAVRLFIEWLKNGGPSSGAPPPS-NH_2), single mutant exendin-4 (H-HGEGTFTSDLSKQ**X**EEEAVRLFIEWLKNGGPSSGAPPPS-NH_2) where **X** is the non-natural amino acid azidohomoalanine (AHA) for fluorescent labeling, and Lys^{40}(^{111}In-DTPA) exendin-4 (H-HGEGTFTSDLSKQMEEEAVRLFIEWLKNGGPSSGAPPPS-Lys(DTPA)-NH2) where DTPA is diethylenetriaminepentaacetic acid for ^{111}In radiolabeling, were custom synthesized from Innopep (San Diego, CA). Preparation and characterization of AlexaFluor 647 single mutant exendin (hereon referred to as 647-exendin) and Cy7 single mutant exendin (hereon referred to as Cy7-exendin) was performed following previously published protocols(*1,2*). The DTPA was conjugated to the ε-amino group of the lysine (K40). ^{111}In-Cl_3 for radiolabeling was obtained from Nuclear Diagnostic Products (Rockaway, NJ). All radioactive materials were handled and disposed following MKSCC standard operating procedures. Lys^{40}(^{111}In-DTPA) exendin-4 (1 µg in DMSO) was added to 848 µL of 0.1 M MES (2-(N-morpholino)ethanesulphonic acid) buffer, pH 5.5. with 1.31 mCi ^{111}In-Cl_3 (48 MBq, 50 µL), resulting in a total volume of 900 µL of the reaction mixture, maintained at a pH of 5.5. The reaction mixture was vortexed at room temperature (20° C) for 30 min. (B) Instant thin layer chromatography (iTLC) of reaction mixture shows >95% exendin radiolabeling. Formation of Lys^{40}(^{111}In-DTPA) exendin (hereon referred to

as 111In-exendin) was monitored using an instant thin-layer chromatography (iTLC) using silica gel plates from Sigma-Aldrich (Milwaukee, WI). 40 mM EDTA at pH 5.5 was used as the mobile phase, and purity/yield was assessed based on the retention distance (Rf). Under these conditions, >95% radiolabeling was achieved and the quality control was performed using instant thin-layer chromatography (iTLC).

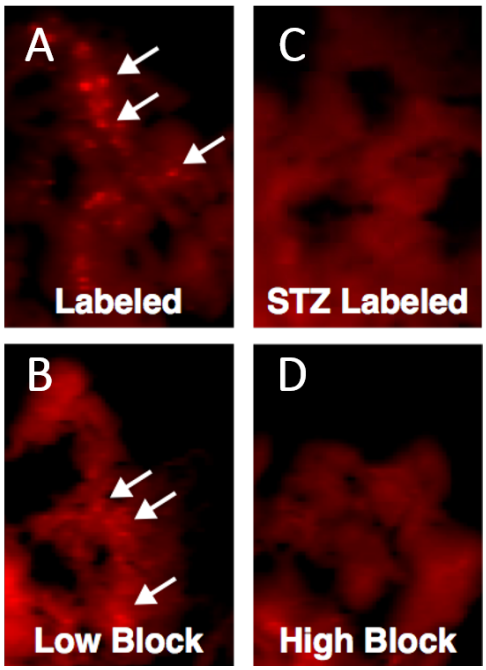

Supplemental Figure 2. Whole organ fluorescence imaging of healthy 647-exendin mice showing presence of punctate signal from islets in (A) label pancreas and (B) low block pancreas, but not in (C) STZ-diabetic labeled pancreas and (D) high block pancreas.

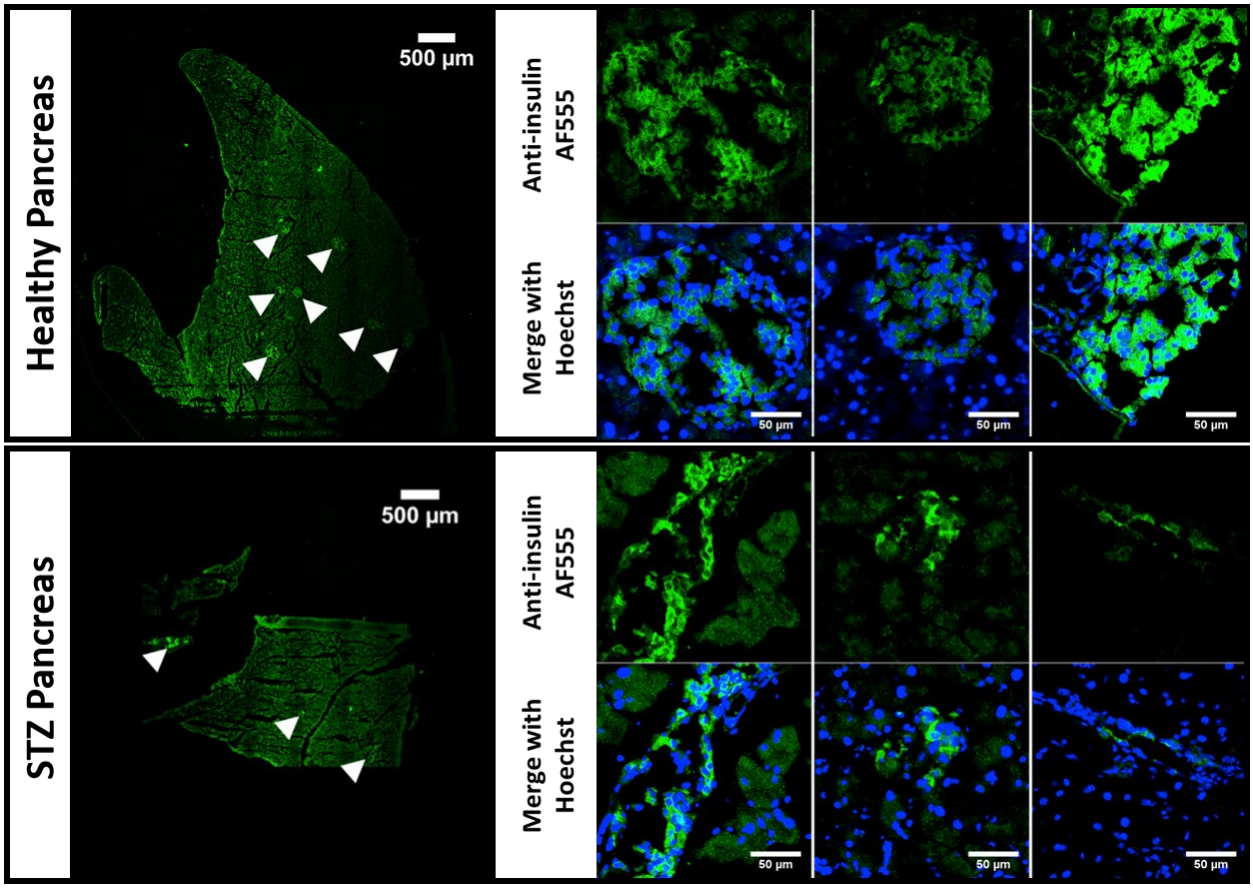

Supplemental Figure 3. Reduced insulin-expressing islets in STZ-diabetic mice. Histology slices of healthy and STZ-diabetic pancreases stained with an AF555-labeled anti-insulin antibody shows an abundance of large, insulin-positive islets (~50-200 µm) in the healthy pancreas compared to the smaller, scarce insulin-positive islets (~20-100 µm) in STZ diabetic pancreas.

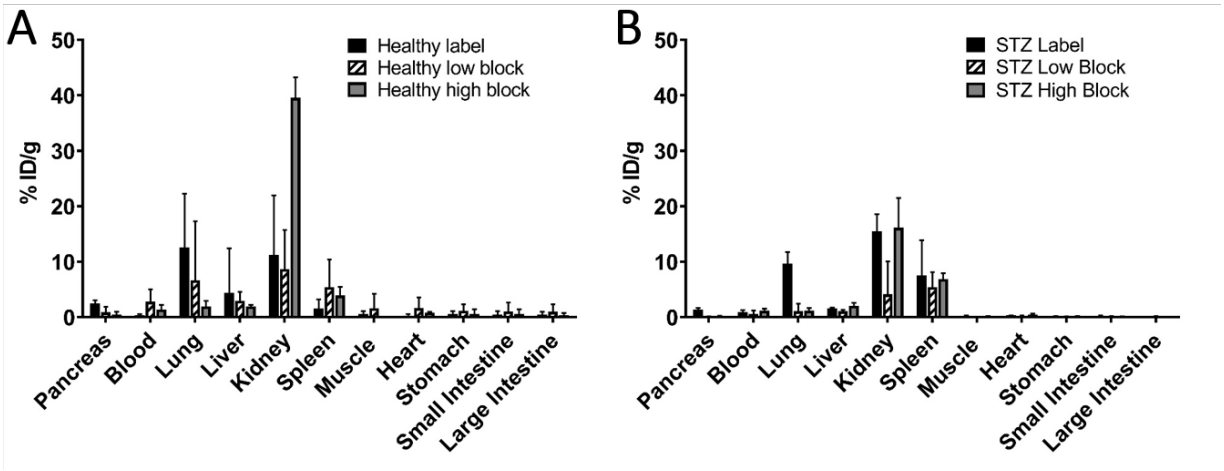

Supplemental Figure 4. Systemic accumulation of radiolabeled exendin represented by biodistribution analysis of radiolabel exendin dose in other mouse organs. Interestingly, the progressively decreasing trend in uptake in healthy pancreata was also observed in healthy and STZ-diabetic mice lungs, consistent with the localization of exendin probes in lungs due to GLP-1R expression(*3,4*). Since GLP-1R is also expressed in human lungs(*4*), this selective blocking strategy could provide the additional benefit of reducing clinical radiotoxicity from off-target 111In-exendin uptake in lungs.

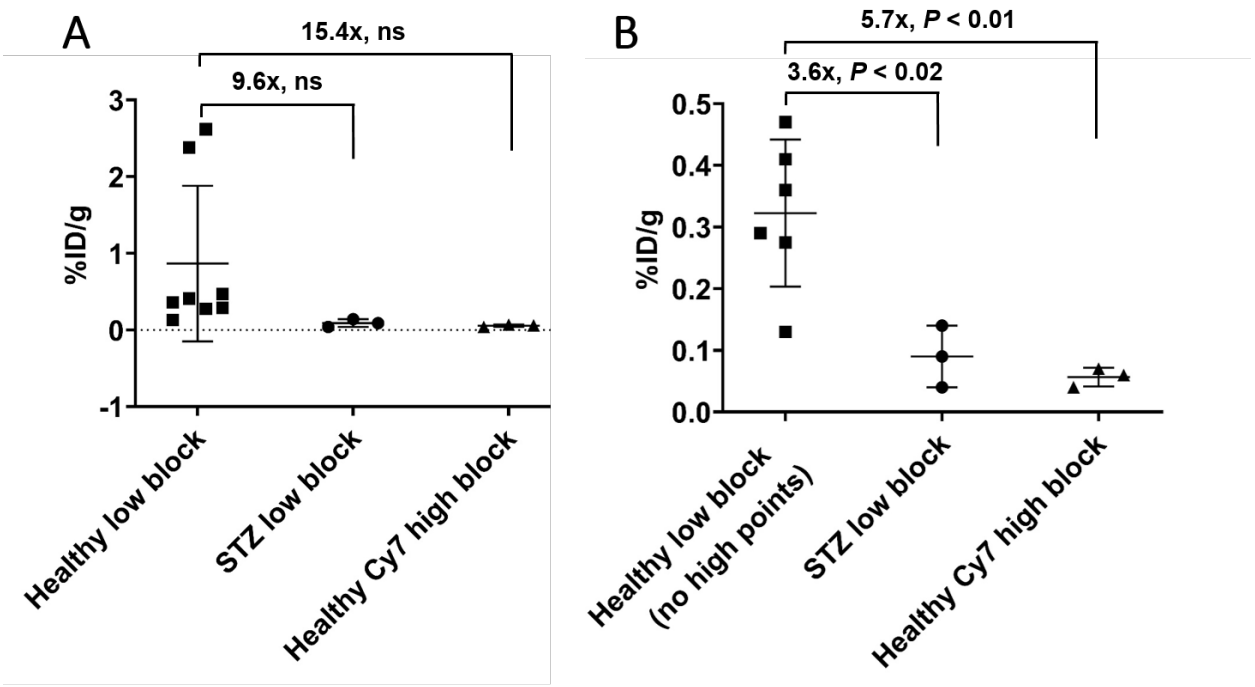

Supplemental Figure 5. 111In-exendin uptake in healthy low block compared to STZ low block and healthy Cy7-exendin high block. (A) The %ID/g of the healthy low block, though higher than STZ low block and healthy Cy7-exendin high block, is not statistically significant. This is due to the large standard deviation of the healthy low block data wherein two data points show high uptake of 111In-exendin (~2.5 %ID/g) in the pancreas, which is consistent with the expected result from blocking all exocrine pancreas but not as many β-cell GLP-1R. Since the Cy7-exendin pre-block dose was estimated to err on the side of complete exocrine blocking, the other uptake data points in healthy low block mice were ~0.3 %ID/g. This large variability precludes the data from showing statistical significance. (B) Without the two high uptake data points, the healthy low-block data is statistically higher than both STZ low block (3.6-fold, $P < 0.02$) and healthy Cy7-exendin high block (5.7-fold, $P < 0.01$), compared to 1.7-fold for label.

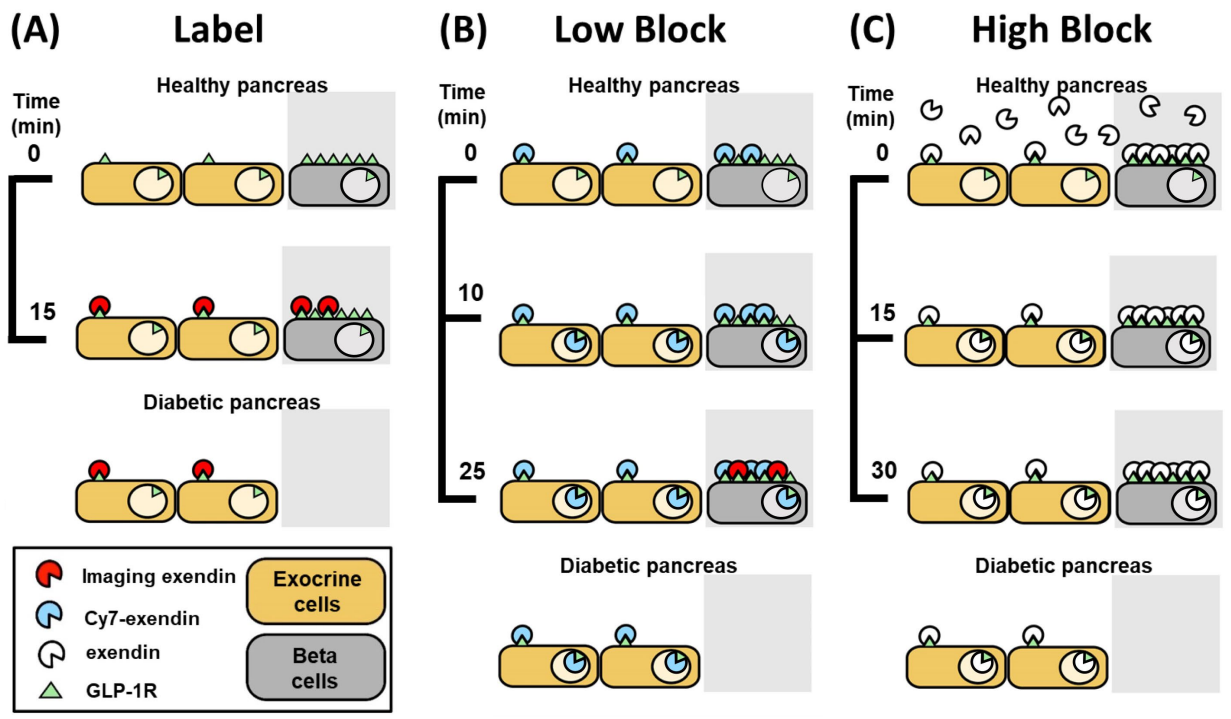

Supplemental Figure 6. Schematic detailing mechanism of selective blocking with lipophilic Cy7-exendin including internalization. (A) When an imaging dose is administered directly ('Label'), it can bind to GLP-1R on both exocrine and β-cells. This explains the higher than anticipated uptake in long-term diabetics who should lack any β-cells, complicating the use of exendin for β-cell imaging. (B) Administration of a small lipophilic pre-block dose ('Low block') provides a potential solution to this challenge by selectively blocking all exocrine GLP-1R while leaving enough β-cell GLP-1R available for binding to the imaging probe. The lipophilicity of the pre-block probe provides several advantages – first, its interaction with plasma proteins enables slower clearances, allowing it to accumulate for longer in the pancreas and block all exocrine GLP-1R as they are trafficked in and out of cells. Second, the slower diffusion prevents the blocking dose from diffusing into and blocking islets from surrounding exocrine, enhancing the selectivity of exocrine GLP-1R blocking. (C) Cold-dose blocking with unlabeled exendin (15-fold more than imaging probe) blocks all available GLP-1R, preventing any uptake of the imaging exendin, and serves as a negative control.

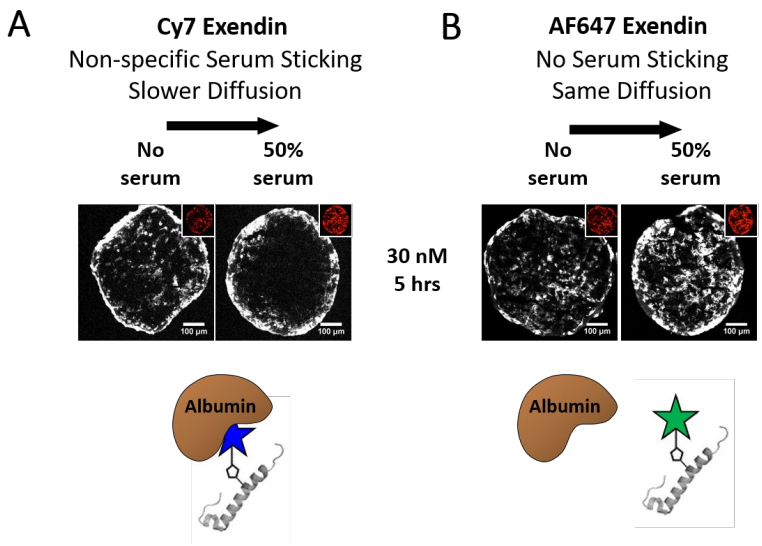

Supplemental Figure 7. Lipophilicity of Cy7-exendin enhances selective blocking of exocrine GLP-1R. (A) Diffusion of lipophilic Cy7-exendin and (B) hydrophilic 647-exendin in GLP-1R positive (inset) spheroids. Theoretical estimates postulate 3-fold higher delivery and uptake in islets compared to exocrine pancreas, due to 3-fold better blood surface area (500 cm^2/cm^3 in islets vs 180 cm^2/cm^3 in exocrine), but ex vivo histology shows almost 5-fold higher uptake(*5*), suggesting that diffusion of the inherently hydrophilic exendin into islets from surrounding exocrine is also a contributing factor. Hydrophilic exendin attains rapid kinetic equilibration, so binding affinity becomes the major factor that determines blocking of exocrine vs β-cell GLP-1R. However, since the binding affinity of exendin to exocrine and β-cell GLP-1R is identical, a hydrophilic exendin cannot achieve selective blocking of exocrine GLP-1R over β-cell GLP-1R. Conjugation of a lipophilic moiety could slow the diffusion of the pre-block dose from exocrine to islets due to plasma protein sticking(*2*). HEK-293 cells transfected with GLP1R-GFP(*2*) were used to grow spheroids in custom-made 384-well plates developed previously(*6*) using the hanging drop method. Details on spheroid culture, processing, and imaging conditions can be provided on request. Diffusion of Cy7-exendin (lipophilic) and 647-exendin (hydrophilic) in the presence and absence of serum proteins in 3D spheroid cultures confirmed that unlike 647-exendin, which diffused throughout the spheroid regardless of the presence or absence of serum, Cy7-exendin showed a remarkably different distribution profile. In the absence of serum, Cy7-exendin diffused throughout the spheroids, similar to 647-exendin (200-250 µm from the edge of the spheroid). However, in the presence of 50% serum, Cy7-exendin only stained the rim (50-100 µm from the edge), despite GLP-1R expression throughout the spheroid (red inset). This is consistent with non-specific sticking of the lipophilic Cy7 moiety to serum proteins, which slows the inherently fast diffusion expected from a small peptide like exendin, supporting the hypothesis that the use a lipophilic pre-block slows the diffusion of exendin from exocrine to islets, thereby enhancing the selectivity of exocrine GLP-1R blocking.

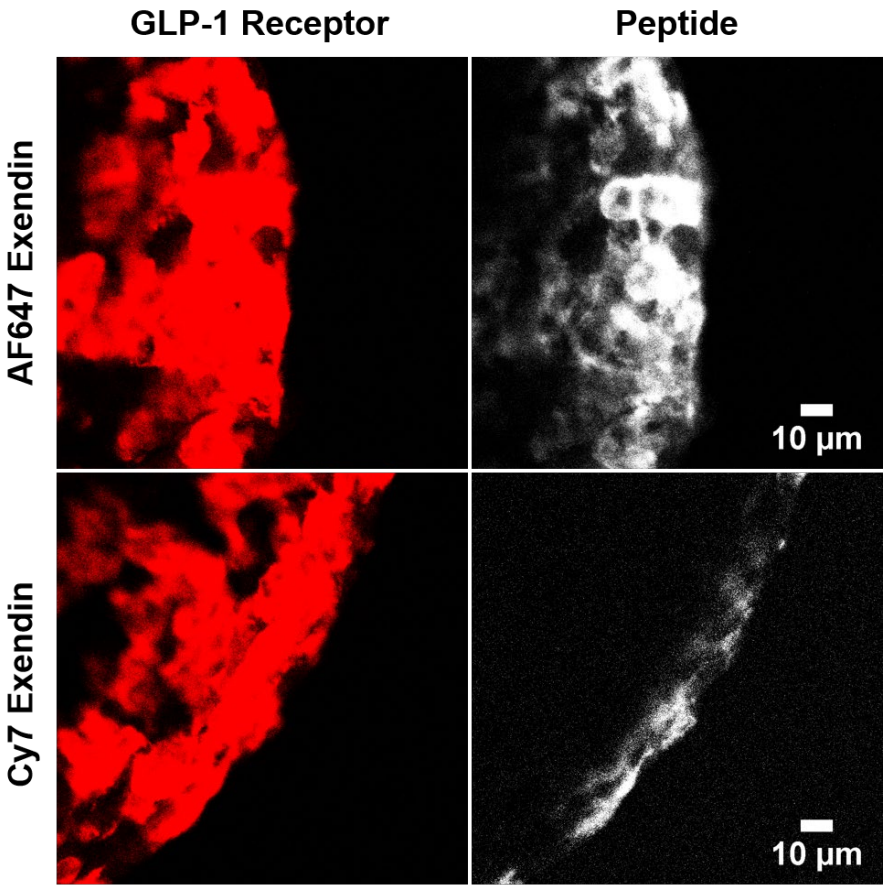

Supplemental Figure 8. High magnification confocal imaging of the edge of HEK293-GLP-1R spheroids pulsed with 10 nM (the estimated concentration of the low-block dose in the pancreas) of either hydrophilic AF647-exendin or lipophilic Cy7-exendin for 10 min (similar time scale as *in vivo* pulse) to estimate how far the peptides diffuse into tissue. Hydrophilic AF647-exendin can diffuse approximately 70 µm from the edge of the spheroid within 10 minutes in the presence of serum, equivalent to diffusing to the center of a 140 µm diameter islet, which is similar in size to mouse islets. Lipophilic Cy7-exendin however, does not diffuse beyond the first cell layer, indicating minimal exposure beyond the outer edge.

Supplemental Table 1. Specific activity of 111In-exendin injected dose.

Healthy				STZ			
Mouse	**Quantity peptide(μg)/50μL**	**Activity (μCi)**	**Specific activity (MBq)/nmol**	**Mouse**	**Quantity peptide(μg)/50μL**	**Activity (μCi)**	**Specific activity (MBq)/nmol**
Label				Label			
1	0.0021	0.87	69.9	1	0.002	0.24	20.2
2	0.0021	0.69	55.4	2	0.002	0.2	16.9
3	0.0021	0.69	55.4	3	0.002	0.22	18.6
Low block				Low block			
1	0.002	1.5	126.5	1	0.002	1.07	90.3
2	0.002	1.08	91.1	2	0.002	1.08	91.1
3	0.002	1.1	92.8	3	0.002	7.45	628.5
1	0.002	1.4	118.1	High block			
2	0.002	1.3	109.7	1	0.002	0.21	17.7
3	0.002	1.3	109.7	2	0.002	0.2	16.9
1	0.002	8.65	729.7	3	0.002	0.2	16.9
2	0.002	9.16	772.7				
3	0.002	8.2	691.8				
High block							
1	0.0021	0.63	50.6				
2	0.0021	0.71	57.0				
3	0.0021	0.64	51.4				
Cy7-exendin high block							
1	0.002	0.52	43.9				
2	0.002	0.52	43.9				
3	0.002	0.51	43.0				

References

1. Zhang L, Navaratna T, Thurber GM. A helix-stabilizing linker improves subcutaneous bioavailability of a helical peptide independent of linker lipophilicity. *Bioconjug Chem.* 2016;27:1663-1672.

2. Zhang L, Thurber GM. Quantitative impact of plasma clearance and down-regulation on GLP-1 receptor molecular imaging. *Mol Imaging Biol.* 2016;18:79-89.

3. Monazzam A, Lau J, Velikyan I, et al. Increased expression of GLP-1R in proliferating islets of men1 mice is detectable by [68Ga]Ga-DO3A-VS-Cys40-exendin-4 /PET. *Sci Rep.* 2018;8:748-748.

4. Viby N-E, Isidor MS, Buggeskov KB, Poulsen SS, Hansen JB, Kissow H. Glucagon-like peptide-1 (GLP-1) reduces mortality and improves lung function in a model of experimental obstructive lung disease in female mice. *Endocrinology.* 2013;154:4503-4511.

5. Eriksson O, Rosenström U, Selvaraju RK, Eriksson B, Velikyan I. Species differences in pancreatic binding of DO3A-VS-Cys40-Exendin4. *Acta Diabetol.* 2017;54:1039-1045.

6. Tung YC, Hsiao AY, Allen SG, Torisawa YS, Ho M, Takayama S. High-throughput 3D spheroid culture and drug testing using a 384 hanging drop array. *Analyst.* 2011;136:473-478.